Applied Catalysis B: Environmental 162 (2015) 45–56

Contents lists available at ScienceDirect

Applied Catalysis B: Environmental

journal homepage: www.elsevier.com/locate/apcatb

Effect of gold on catalytic behavior of palladium catalysts in hydrodechlorination of tetrachloromethane

Magdalena Bonarowska[a], Zbigniew Kaszkur[a], Dariusz Łomot[a], Michał Rawski[b], Zbigniew Karpiński[a,c,*]

[a] Institute of Physical Chemistry of the Polish Academy of Sciences, ul. Kasprzaka 44/52, PL-01224 Warszawa, Poland
[b] Faculty of Chemistry, Analytical Laboratory, Maria Curie-Skłodowska University, Plac Marii Curie-Skłodowskiej 3, PL-20031 Lublin, Poland
[c] Faculty of Mathematics and Natural Sciences-School of Science, Cardinal Stefan Wyszyński University, ul. Wóycickiego 1/3, PL-01938 Warszawa, Poland

ARTICLE INFO

Article history:
Received 21 March 2014
Received in revised form 26 May 2014
Accepted 6 June 2014
Available online 13 June 2014

Keywords:
Pd-Au/C
CCl_4 hydrodechlorination
Synergy
Selectivity for hydrocarbons
Effect of HNO_3 dissolution

ABSTRACT

Catalytic gas-phase hydrodechlorination (HdCl) of tetrachloromethane was investigated over Au/Sibunit and Pd/Sibunit carbon prepared by impregnation, and Pd-Au/Sibunit carbon prepared by either reductive deposition of Au onto Pd or successive impregnation of Pd/Sibunit carbon with a solution of gold salt carried out at aerobic conditions. The activated (by reduction in H_2 at 400 °C) catalysts were characterized in terms of H_2 and CO chemisorptions, XRD and (S)TEM-EDS measurements. Presence of smaller (<2 nm) metal particles in 2.8 wt.% Pd/Sibunit (d_{mean} 3.1 nm) evidenced by TEM was not confirmed by XRD and gas chemisorptions. XRD and (S)(TEM)-EDS showed a reasonable quality of Pd-Au alloying in catalysts prepared by reductive deposition. Compared with the monometallic palladium, active carbon-supported bimetallic Pd-Au catalysts (~0.24 g charges) showed very good activity (conversions up to 92%), resistance to deactivation during ~70 h runs and high selectivity to nonchlorinated products (up to ~80%) in the reaction of hydrodechlorination of tetrachloromethane, carried out at 90 °C. However, their behavior greatly depends on the quality of Pd-Au alloying: well mixed Pd-Au particles of Pd-Au maintain a very good catalyst performance, while the increasing presence of small unalloyed Pd particles leads to rapid deactivation. A large part of these small Pd particles can be leached out from such insufficiently homogenized catalystsby dissolution in 10% nitric acid. This treatment, followed by catalyst re-reduction results in the remarkable improvement of catalytic performance, especially the catalyst's stability in a long-term operation. During the reaction, carbon species originating from CCl_4 enter palladium (but not PdAu) bulk, leading to the formation of the palladium carbide phase, PdC_x, which seems to be less effective in hydrogen activation, and results in massive accumulation of nonreactive deposits containing both carbonaceous as well as chlorine species leading to rapid catalyst deactivation.

1. Introduction

Catalytic hydrodechlorination (HdCl) appears to be one of the most prospective technologies for the utilization of harmful chlorine-containing wastes [1,2]. In contrast to incineration and catalytic burning, HdCl offers conversion of toxic and ozone-depleting substances to more benign while still valuable chemicals. Until recently, HdCl of tetrachloromethane to chloroform carried out in the presence of Pt-based catalysts was regarded as a suitable practice [3–5], but today because of its high toxicity and carcinogenic character $CHCl_3$ is included in the U.S. EPA's Toxic Release Inventory (TRI). Thus, conversion of CCl_4 to chlorine-free compounds, i.e. hydrocarbons, appears now a more prospective solution. Compared to platinum, palladium catalysts were found more useful in such a transformation [6–15], however they quickly deactivate on stream [6–9,12–16].

It seems general consensus that small metal (Pt, Pd) particles are less suited for HdCl, both in batch liquid and continuous gas phase operations (Refs. [17–27], for Pd catalysts). Small metal particles strongly deactivate [3,5], especially when they interact with support acidity, becoming electrodeficient [5]. It appears that the more acidic support, the faster catalyst deactivation. In this respect, basic MgO appears a better support than Al_2O_3, although still is not good, quickly deactivating on stream [8]. In addition, possible transformation of basic supports to respective chlorides during HdCl would lead to catalyst's downgrading, since MgO

* Corresponding author at: Institute of Physical Chemistry of the Polish Academy of Sciences, ul. Kasprzaka 44/52, PL-01224 Warszawa, Poland.
Tel.: +48 3433356; fax: +48 3433333.
E-mail address: zkarpinski@ichf.edu.pl (Z. Karpiński).

http://dx.doi.org/10.1016/j.apcatb.2014.06.007
0926-3373/

turns $MgCl_2$, reducing the surface area [28]. Carbon is the support of industrial choice for a number of reasons, including high specific surface area, availability and stability against corrosion by chlorine-containing species, and, in effect, Pd/active carbon catalysts were intensively investigated. Gómez-Sainero et al. [29] suggested that both electrodeficient and zero-valent species are needed for HdCl of CCl_4 on carbon-supported Pd catalysts in gas phase, whereas catalysts with only one of the species ((Pd^{n+} or Pd^0) are inactive. They proposed a dual nature of Pd active sites by the association of both species, reaching a maximum of activity at a Pd^{n+}/Pd^0 ratio close to 1. Other authors were also in agreement with the proposed dual nature of the Pd active sites in HdCl [23,25,30–32]. Concerning the electronic effects, Diaz et al. [25] admit that there are not a clear relationship between dispersion and concentration of electro-deficient palladium species (as judged from XPS), being this parameter markedly more dependent on the considered support and the surface activation than on the metal dispersion itself. Therefore, sources of electrodeficiency of carbon-supported palladium particles would be seen in the extent of Pd interactions with oxygen-containing (acidic) functional groups present on carbons, which were not subjected to a sufficiently rigorous temperature pretreatment, especially in a reducing atmosphere (H_2).

Reasons for deactivation of HdCl metal catalysts are at least threefold. First, metal surface chloriding by a liberated HCl product was thought to be an important cause of deactivation [33–36]. Second, perhaps a more frequently evoked cause, considers massive deposition of carbonaceous deposits blocking the active metal sites [37–40]. Third, changes in the metal phase, such a decrease of metal dispersion caused by long-term operation in this highly exothermic reaction, were also suggested to play an important role in the time-on-stream behavior of HdCl catalysts [41]. Finally, a combination of the previously mentioned factors, e.g. chlorination + carbiding, may also be taken into account [42,43]. So far, regeneration of palladium catalysts subjected to HdCl of CCl_4 was not very successful, giving only a short-lived or partial recovery, no matter how was carried out (high temperature flushing with inert gas [9,38] or burning post-reaction deposits [43]). This limitation reinforces our determination to develop long-lasting catalysts of HdCl of CCl_4.

At this stage of research, modification of an active phase (Pd) appeared to us a better way to improve the HdCl performance than concerns about possible benefits from support selection. So, we decided to modify carbon-supported palladium particles with gold, i.e. to investigate the system which frequently was found to exhibit synergy in the catalytic behavior. Synergistic effects observed for Pd-Au alloys are interpreted by occurrence of two effects: ensemble (geometric) and ligand (electronic) ones. The ensemble effect is a dilution of surface Pd by Au, leading to disappearance of contiguous Pd site ensembles and creation of isolated Pd sites. In their recent review, Gao and Goodman [44] argued that for vinyl acetate synthesis, this effect is responsible for reaction rate and selectivity enhancements via the formation of highly active surface sites, e.g., isolated Pd pairs. The ligand effects occuring via direct charge transfer or by affecting bond lengths, cause the Pd d band to be more filled, moving the d-band center away from the Fermi level. This makes Pd more “atomic like” which binds reactants and products more weakly. For certain reactions, this relieves catalyst deactivation caused by self-poisoning and enhances activity/selectivity. Such effect would explain better resistance to deactivation of Pd-Au alloys. Venezia et al. [45] reported a synergetic effect of gold in Au/Pd catalysts in HDS reactions, seen as a stronger resistance of gold to sulfur poisoning and to the ensemble size change of the alloyed phase. A more relevant for this study improvement of deactivation resistance in HdCl (of mainly trichloroethene) reactions by for gold-supported palladium nanolayers was observed in numerous papers from the group of Wong [46–53]. In the last paper, on HdCl of $CHCl_3$, Au/Al_2O_3 catalysts modified by deposition Pd appeared much more active than respective Pd/Al_2O_3 catalysts, suggesting a close vicinity of Pd (or at least some part of it) and Au. In general, in a majority of Wong et al. papers both ensmble and ligand effects are invoked to describe the superiority of Pd-Au combinations. Wu et al. [54] reported the catalytic behavior of a magnetic core–shell nanocomposite, Fe_3O_4@SiO_2@Pd-Au, which was synthesized by reducing palladium and gold cations previously bound to the amine ligand-modified surface of silica-encapsulated iron oxide (Fe_3O_4) nanoparticles. The formation of a Pd-Au alloy resulted in an enhanced 4-chlorophenol conversion and better catalyst’ stability, whereas the presence of magnetic iron oxide was considered to facilitate catalyst separation from liquid reaction mixture. Pd-Au/Sibunit catalysts were found more selective to CH_2F_2, desired product in HdCl of CCl_2F_2 [55]. It should also be mentioned that, due to the possibility of the occurrence of synergistic effects in catalytic behavior, the Pd-Au system maintains an object of continuing interest [56–58].

Modification of palladium (which is generally regarded as an active phase in HdCl reactions) by alloying with other than gold catalytic metals also upgraded the catalytic performance. Golubina et al. showed that iron addition to palladium greatly increases the catalyst’s life time and also leads to a better selectivity towards C_2–C_4 hydrocarbons [59]. Addition of silver or copper to palladium also had a beneficial effect on the catalytic behavior in HdCl of 1,2-dichloroethane, resulting in higher selectivity to ethene (desired product) [60–65]. However, in the case of HdCl of CCl_4 such modifications brought about less preferred changes because either the product selectivity was turned towards chloroform and not to preferred hydrocarbons (Pd-Ag, [66]) or the catalyst stability was not good (Pd-Cu, [67]). Interestingly enough, modification of Ni catalysts by Au generated synergistic effects in HdCl of 2,4-dichlorophenol [68].

In this report we present new data on the behavior of active carbon-supported Pd-Au catalysts in HdCl of CCl_4. Practical reasons prompted us to investigatethe catalysts under the conditions of (nearly) full CCl_4 conversion achieved at possibly lowest temperatures of reaction.

2. Experimental

2.1. Catalysts preparation and characterization

The support was Sibunit carbon [69] in the form of powder (grain size between 10 and 30 μm), washed with a boiling mixture of concentrated HCl and HF purged with redistilled water and dried in an air oven. Its nitrogen BET surface area measured with an ASAP 2020 Micromeritics instrument was 390 m^2/g, BJH pore volume (from desorption branch) was 0.75 cm^3/g, and average pore diameter was ~7 nm. The cumulative micropore volume (Horvath–Kawazoe) was 0.11 cm^3/g, as estimated at relative pressure 0.012, and the median micropore diameter was 0.59 nm.

First, the primary monometallic 2.8 wt.% Pd/Sibunit was prepared by incipient wetness impregnation using an aqueous solution of $PdCl_2$ (analytical grade from POCh Gliwice). An anaerobic sequential impregnation method was used to prepare Sibunit carbon-supported Pd-Au catalysts. The monometallic Pd/Sibunit catalyst was prereduced at 300 °C for 3 h in a special reactor in flowing H_2–Ar (300 cm^3/min), then purged in an argon flow at 300 °C for 1 h, cooled to room temperature in Ar, and, finally, immersed in de-aerated redistilled water. The solution was continuously stirred by bubbling argon, at 200 cm^3/min. Then, a de-aerated aqueous solution of ammonium chloroaurate (specpure from Johnson Matthey, England) was slowly introduced into the reactor. The solution was stirred with bubbling argon for the next 20 min. The resulting solid was separated by filtration, washed with redistilled water, and

Table 1
Characteristics of Pd-Au/Sibunit carbon catalysts.

Catalyst[a]	Metal dispersion		Conclusions from XRD and TEM
	CO/Pd[b]	H/Pd[c]	
2.8 wt.%Pd100	0.20	0.13	TEM: rather narrow particle size distribution: $d_{TEM} \approx 3.1$ nm, $d_{XRD} \approx 5$ nm
6.2 wt.%Pd60Au40-SI	0.11	0.11	XRD and TEM: big Pd10Au90 particles (~20 nm) + small Pd particles (~3 nm).
4.1 wt.%Pd82Au18-RD	0.10	0.05	XRD: Pd50Au50 (8.2 nm), 64%; Pd100 (12 nm), 36%
4.9 wt.%Pd71Au29-RD	0.08	0.04	XRD: Pd60Au40 (8.1 nm), 80%; Pd100 (6.7 nm), 20%
6.0 wt.%Pd62Au38-RD	0.07	0.05	XRD: Pd50Au50 (6 nm), ~90%; Pd100 (7.5 nm), ~10%; TEM-EDS: good PdAu intermixing, small amount of Pd particles (~5–7 nm)
7.9 wt.%Pd49Au51-RD	0.09	0.06	TEM: broad particle size distribution (2.5–25 nm), small Pd100 and larger ~Pd35Au65 particles

[a] In the notation *W* wt.% PdXAuY-RD/SI, W represents overall metal (Pd + Au) weight loading. *X* and *Y* denote atomic percentages of Pd and Au. RD or SI stands for sequential reduction deposition or sequencial incipient wetness impregnation of gold salt, respectively (see Experimental).
[b] From static chemisorption of CO at 35 °C.
[c] From pulse-flow chemisorption of H_2 at 70 °C.

dried in flowing argon at 60 °C for overnight, and finally stored in a desiccator. This series of Pd-Au/C catalysts were designated as "RD", i.e. reductive deposition. One Pd–Au/Sibunit catalyst were prepared by introduction of the gold salt into 2.8 wt.% Pd/C by sequential incipient wetness impregnation ("SI"). Weight loadings of palladium and gold were determined by atomic absorption spectroscopy (AAS). Chlorine content in activated catalysts was not determined. Our previous work with Sibunit impregnated with $NiCl_2$ showed negligible chlorine content after reduction in H_2 at 400 °C [70]. Similarly, Gurrath et al. did not see any chlorine in Pd/C catalysts prepared from $PdCl_2$ and subjected to reduction at the same temperature [71]. Two Au/Sibunit catalysts of 2 and 3 wt.% metal loadings were prepared incipient wetness impregation of ammonium chloroaurate.

Designation of all prepared catalysts is in Table 1. The catalysts were also characterized by H_2 and CO chemisorption, XRD, TEM (selected samples) and temperature-programmed studies. CO adsorption was measured at 35 °C in a static system, using a double isotherm method (ASAP 2020 instrument from Micromeritics). Irreversible uptake of hydrogen was measured in a pulse-flow method system at 70 °C, in order to avoid the formation of β-PdH, as described in [55]. H_{ad}/Pd_t and CO_{ad}/Pd_t ratios were taken as measures of apparent metal dispersion. Prior to characterization, the catalysts were pretreated in the same way as before kinetic experiments (next subsection), i.e. with the final reduction in hydrogen at 400 °C for 2 h.

Reduced and post-reaction catalyst samples were investigated by X-ray diffractometry (Rigaku Denki, Ni-filtered CuK_α radiation). The obtained XRD profiles were fitted to an analytical function of the PEARSON-VII type using commercial PEAKFIT software. For phase identification and calculation of the phase composition, centroids of the fitted profiles were used, and for the calculation of the crystallite size, the half-widths of the fitted profiles were taken. High resolution bright-field TEM (HRTEM) and high angle annular dark field imaging in scanning mode TEM (HAADF-STEM) of the metallic particles was performed using TITAN Cubed FEI electron microscope with accelerating voltage of 300 kV. The condensed beam analyzed using X-ray energy-dispersive spectrometer in TEM mode and EDS with energy resolution 134 eV scanning in HAADF-STEM mode using EDAX detector allowed to estimate the local concentration of chemical elements. At least a hundred particles were employed to compose the histogram of size distribution defined by the number of particles with a given size. Above 10–15 localities have been sampled in each specimen using TEM and STEM.

Post-reaction catalyst samples were also investigated by temperature programmed hydrogenation (TPH-MS). TPH-MS runs were carried out in a flowing 10%H_2/He mixture (25 cm^3/min) at a 10 °C/min ramp and followed by mass spectrometry (MA200, Dycor-Ametek, Pittsburgh, USA). Principal attention was paid to *m*/*z* 15 and 16 (methane evolution), and *m*/*z* 36 and 38, which are suggestive of HCl liberation from catalysts used. The same reaction system was used for temperature programmed desorption from reduced Pd-Au/Sibunit catalyst which were subjected to nitric acid treatment at room temperature for a period of 10 or 20 h. Amounts of desorbed CO_2 and CO were taken as a relative measure of carbon support acidity, associated with possible occurrence of oxygen-containing functional groups.

2.2. Hydrodechlorination of tetrachloromethane

Prior to the reaction, the catalyst charge (always ~0.24 g) was dried at 120 °C for 0.5 h in an argon flow and reduced in flowing 20% H_2/Ar (25 cm^3/min), ramping the temperature from 120 °C to 400 °C (at 8 °C/min) and kept at 400 °C for 2 h. The reaction of HdCl of tetrachloromethane (analytical reagent from POCh, Gliwice, Poland, stated purity 99.6%, practical purity 99.9%), provided from a saturator maintained at 0.0 °C (±0.1 °C) and bubbled in a flow of H_2/Ar mixture (29 cm^3/min), was carried out at 90 °C and the H_2:CCl_4 ratio ~14:1, in a glass flow system, as previously described [20,44,53]. The flows of H_2 and Ar (all 99.999% pure, further purified by passing through MnO/SiO_2 traps), were fixed by using MKS mass flow controllers. The partial pressures of the reaction mixture were: CCl_4 4.3 kPa, H_2 60.5 kPa, Ar 36.5 kPa. Contact time (V/F) ~0.5 s was applied. The reaction (at 90 °C) was followed by gas chromatography (HP 5890 series II with FID, a 5% Fluorcol/Carbopack B column (10 ft) from Supelco). HCl evolution, to check the chlorine balance, was not monitored. After screening at 90 °C and reaching a steady state, the temperature was gradually decreased to 80 °C and 70 °C, and new experimental points were collected Finally, the reactor was heated to 90 °C, and, in nearly all cases, the previous results collected at 90 °C were restored. A typical run lasted ~70 h. The agreement in final conversion was fair, ±5%. Much better repeatability was found for product distribution, where final selectivities toward major products were in good agreement ±2%. Since all catalyst charges (~0.24 g) contained nearly identical amounts of palladium, the conversion level of CCl_4 was the first direct measure of catalytic activity per g_{cat} or per g_{Pd}.

Very small catalyst grains (10–30 μm) allow us to neglect the possibility of internal diffusion limitations, which were found to play a role in the HdCl of 1,2-dichloroethane on carbon-supported Pd-Ag catalysts [50]. However, the cited authors disposed with much larger catalysts grains (≥250 μm). Moreover, their catalysts characterized by the smallest grains showed the effectiveness

factor equal 1 or very close to 1. On the other hand, disposing with so highly powderized catalytic material would not undertake respective studies with still smaller than ours catalyst' grains. The effect of external diffusion was checked for the 6.0 wt.% Pd62Au38-RD catalyst which exhibited very high final conversion level. For keeping the contact time ($Vcat/F_{CCl4}$) unchanged, we took half of the standard catalyst's charge and two times lower flow of the reaction mixture, while keeping its composition unchanged. Fairly good agreement in the time on stream behaviors for both cases, especially, similar final conversions (i.e. ~5% lower for the lower CCl_4 flow) and nearly identical product distributions. Therefore, it appears that internal and external transport effects do not contribute to HdCl performance at our conditions.

The bimetallic catalysts which exhibited a limited degree of Pd-Au alloying showed a severe deactivation in time on stream (*vide infra*). Unalloyed palladium was decided to leach out from these samples by treating them with a 10% nitric acid, followed by careful wash with redistilled water until pH 7, drying and re-reduction in hydrogen at 400 °C. Such pretreated catalysts were analyzed by AAS, ICP, XRD, and screened in the HdCl of CCl_4.

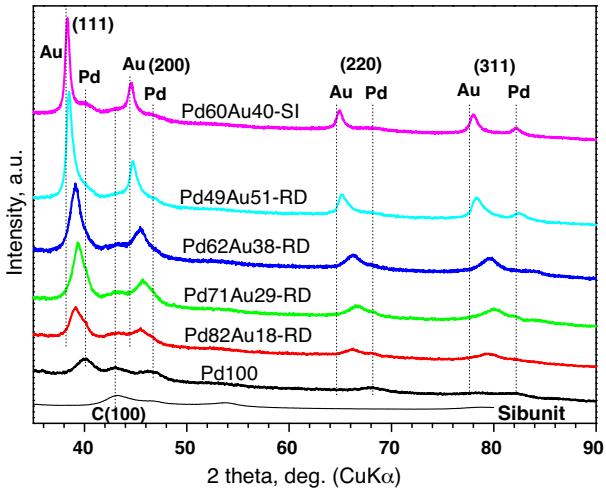

Fig. 1. XRD profiles of reduced Sibunit carbon-supported Pd-Au catalysts. For catalyst designation see text. Basic XRD reflections from palladium and gold are marked. Bottom thin line represents the diffractogram from Sibunit carbon support.

3. Results and discussion

3.1. Catalyst characterization

Figs. 1–4 and collectively Table 1 show the results of XRD, TEM and chemisorption studies performed on Pd and Pd-Au/C catalysts. The dispersion value of Pd100, based on CO chemisorption, corresponds well with the Pd crystallite size assessed from XRD (1.12/(CO/Pd) ≈ 5.5 nm, according to [72]), although agreement with TEM data is rather moderate (3.1 nm, average particle size, Fig. 2b). Apparently underestimated by XRD and CO chemisorption metal dispersion can be explained by either poor XRD detection of smaller (e.g. <2 nm) Pd particles, or a suppressed CO chemisorption, earlier observed for carbon-supported Pd catalysts. Krishnankutty and Vannice [73] found that variously prepared Pd/carbon catalysts displayed good metal dispersion, as shown by TEM and XRD, however, gas (H_2, CO, O_2) chemisorption, especially hydrogen, was substantially suppressed. Similar disagreement between palladium dispersion assessed from CO adsorption and TEM was found by Job et al. (first entry row in Table 2 in [63]). Their 1.4 wt.% Pd/C catalyst showed d_{TEM} = 3.1 nm, whereas CO uptake was 1.62 mmol CO/g_{Pd}, equivalent to the molar ratio CO_{ad}/Pd_t = 0.172, what, according to [72], should reflect the presence of ~6.5 nm Pd particles (1.12/0.172). In another work, Krishnankutty et al. [74] showed that the metal surface of reduced carbon-supported Pd catalysts may be partly contaminated with carbon, leading to a decreased gas chemisorption. This fact would also be responsible for suppression of gas chemisorption in the present work, more pronounced for H_2 than for CO, as it is seen for Pd100 (Table 1).

Pd-Au catalysts showed smaller gas uptakes, only roughly corresponding with metal dispersion judged from XRD and TEM data (Table 1). Again, although with one exception, the CO/Pd ratios were found higher than the H/Pd ones. Similar observations were made by Sárkány et al. [75] who also took direct CO_a/Pd and H_a/Pd ratios as a measure of metal dispersion in their Pd-Au/Al_2O_3 catalysts. They showed that the H_{ad}/CO_{ad} ratio was 0.6–0.7 over monometallic Pd samples, but dropped significantly for the bimetallic (Pd-Au) ones. They invoked two reasons for H_a/CO_a ratio variations. First, due to the corrosive adsorption of CO the number of surface Pd atoms would be overestimated for the Pd-Au samples. The second reason would be that the hydrogen adsorption was performed in a pulse system (dynamic conditions) at 90 °C (in our case 70 °C) to prevent β-PdH formation, so weak hydrogen adsorption sites

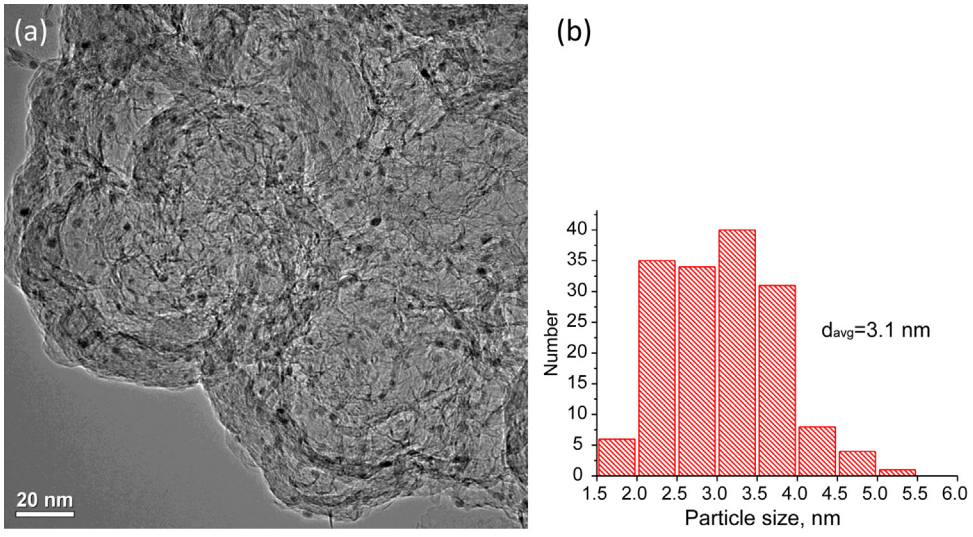

Fig. 2. TEM of Pd/Sibunit: micrograph (a), particle size distribution (b).

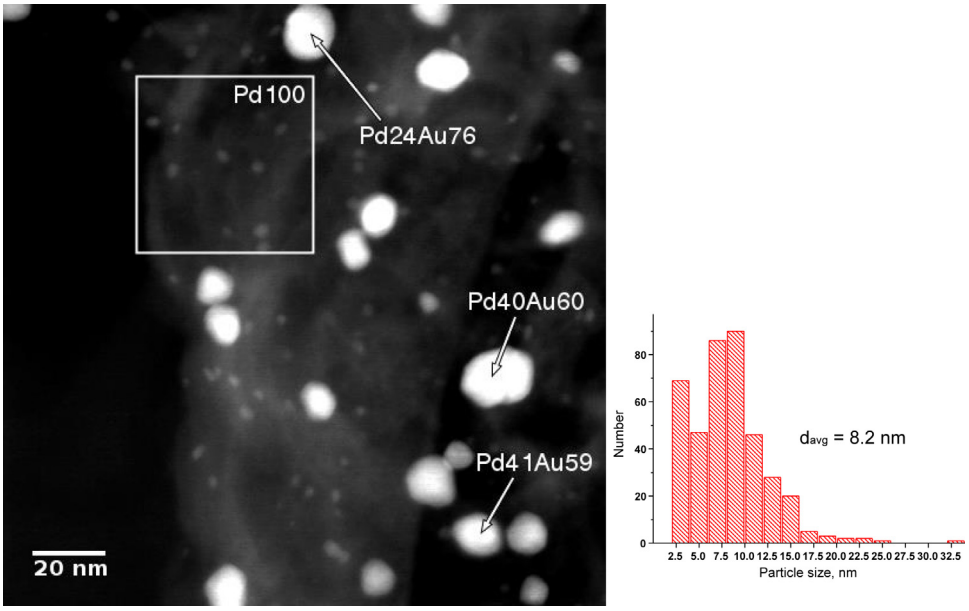

Fig. 3. STEM of Pd49Au51-RD: micrograph (a), particle size distribution (b).

were not observed. Correspondingly, Lam and Boudart [76] found that the H_{ad}/CO_{ad} ratio decreased with increasing Au-to-Pd ratio in silica-supported Pd-Au catalysts.

The quality of metal alloying is the problem of paramount importance in catalysis by bimetallic systems. This factor is estimated here from XRD (Fig. 1) and (S)TEM-EDS (Figs. 3a and 4) results and summarized in the last column of Table 1. Very clear situation was found for Pd60Au-SI (prepared sequential impregnation carried out in air), where two nearly pure Pd and Au phases were indicated by XRD (Fig. 1) and TEM (micrograph not shown), indicating negligible alloying of both metals. Because the number of spots probed by EDS was not very large (10–15 localities, depending on sample), forming the data set which was not statistically significant, our EDS analysis does not allow us to propose a single parameter, which would be regarded as the degree of alloying. Nevertheless, the micrographs in Figs. 3 and 4, selected as the most representative, serve rather for illustration and supporting the XRD results, we believe that they are essential to show the presence of highly dispersed unalloyed Pd particles, which are hardly detected by XRD. Their presence in the bimetallic catalysts will be essential for discussion of catalytic behavior in HdCl of CCl_4 (next subsection). General interpretation of XRD and TEM-EDS studies is that the Pd-Au catalysts prepared by sequential reduction impregnation (RD) are reasonably, although not ideally, alloyed. Some catalysts, i.e. Pd70Au30-RD and Pd60Au40-RD showed quite good alloy homogeneity, with 80–90% of palladium intermixed with gold. In the case of Pd80Au20-RD the situation was not as good, because up to ~36% Pd was left unalloyed. As already mentioned, the poorest situation was found for Pd60Au-SI (sequential impregnation carried out in air), where both XRD and TEM-EDS showed nearly entire separation of both metals (Figs. 1 and 4, and last column in Table 1). Evident contribution of unalloyed palladium was also documented in XRD profiles of post-reaction catalysts. For some Pd–Au/C catalysts a distinct peak asymmetry is distinguished: the right branches of all (111) and (200) lines are noticeably distorted by the presence of unalloyed palladium (Fig. 1). After a longer exposure to the reaction mixture unalloyed palladium (lattice constant ~0.389 nm) is converted to $PdC_{0.13}$ [77], or even to $PdC_{0.15}$ [78] with lattice constant ~0.399 nm, what shifts the (111) XRD reflection to lower diffraction angles (2Θ) by ~1 degree. The occurrence of palladium carbiding during HdCl processes is known [20,55,79–84] but here we notice this effect for the reaction of carbon tetrachloride at a relatively low reaction temperature (90 °C). Due to the difference of lattice constant of Pd and Au, analogous shifts of the XRD reflections go along palladium alloying with gold. So, carbon dissolution in Pd as an effect of the reaction produces more narrow and symmetric diffraction profiles, because the contribution from unalloyed Pd is now hidden in the

Table 2
CCl_4 hydrodechlorination on Pd-Au catalysts. Final conversions, product selectivities, turnover frequencies and activation energies.

Catalyst[a]	Final conversion[b] (%)	Product distribution[b] (%)						TOF[c] (s^{-1})	Activation energy[d] (kJ/mol)[c]
		Hydrocarbons				Chlorocarbons			
		CH_4	C_2H_6	$\Sigma C_{x>2}H_{2x+2}$	ΣC_nH_{2n+2}	$CHCl_3$	$C_2H_yCl_z$		
Pd100	3.2	30.8	6.8	1.3	38.9	3.1	58.0	2.04×10^{-3}	51.9 ± 3.0
Pd60Au40-SI	4.6	59.3	13.0	9.5	81.8	3.4	14.8	5.43×10^{-3}	59.9 ± 5.0
Pd82Au18-RD	38.2	27.2	19.9	29.8	76.9	4.5	18.6	4.75×10^{-2}	38.5 ± 0.5
Pd71Au29-RD	83.6	32.0	21.6	17.3	70.9	6.5	22.5	1.45×10^{-1}	16.5 ± 0.5
Pd62Au38-RD	92.0	37.1	17.8	14.0	68.9	5.7	25.3	1.72×10^{-1}	14.5 ± 1.0
Pd49Au51-RD	58.0	38.7	14.8	18.2	71.7	3.9	24.5	8.60×10^{-2}	39.5 ± 1.0

[a] As in Table 1.
[b] Final conversions and product selectivities after ca.70 h of time on stream (reaction temperature 90 °C).
[c] Turnover frequency (at 90 °C) after ca.70 h of time on stream, based on dispersion data shown in Table 1 (CO/Pd).
[d] Based on overall conversions collected at 70, 80 and 90 °C.

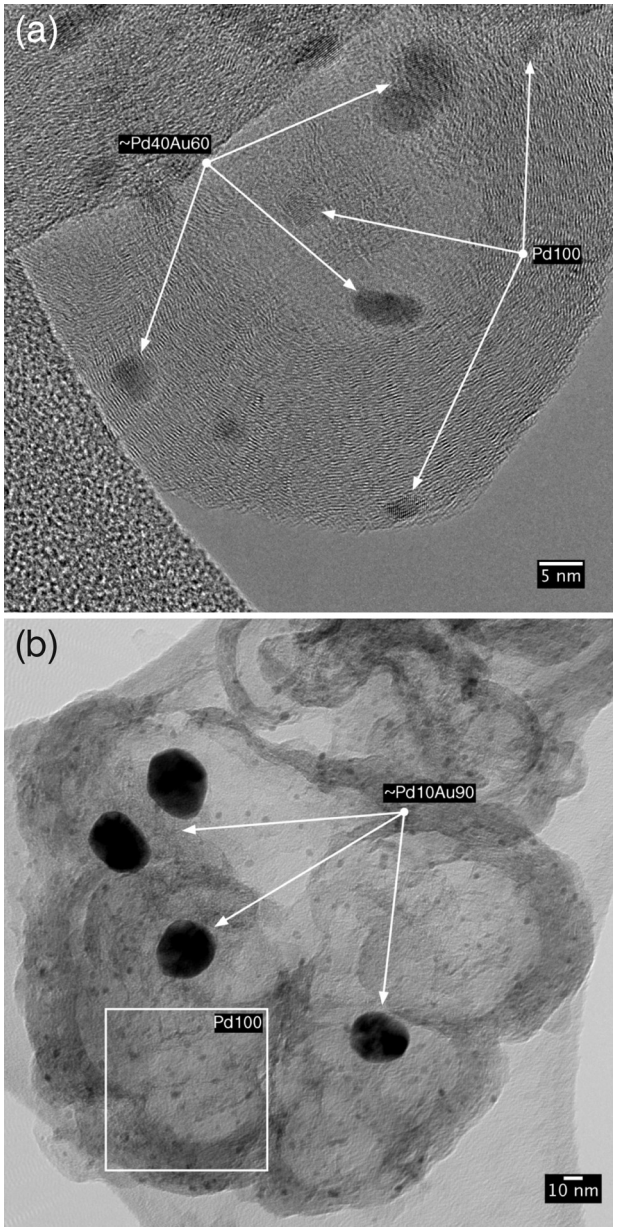

Fig. 4. TEM micrographs of Pd62Au38-RD (a) and Pd60Au40-SI (b).

Pd-Au reflection (Fig. 5). Post-reaction Pd-Au catalysts subjected to subsequent hydrogen treatment at 400 °C restores previous asymmetric (111) reflections, having again their right branches slightly distorted by the presence of unalloyed Pd (XRD lines not presented). This reveals that further Pd-Au alloying does not occur during the above-mentioned transformations, indicating that unalloyed palladium must be separated from a gold-containing material. Because carbiding of well-homogenized Pd-Au alloys is not likely [85], the aforementioned shifts of XRD reflections should be only attached to the presence of unalloyed palladium. This effect will be considered later during discussion on palladium deactivation.

3.2. Catalytic conversion of CCl_4

3.2.1. Time on stream behavior

3 wt.% Au/Sibunit catalyst, subjected to reduction in H_2 at 400 °C (crystallite size ~20 nm by XRD), did not exhibit any CO and H_2 irreversible chemisorption and was almost completely inactive at 90 °C (conversion < 0.2%) at 90 °C, which was selected as the highest

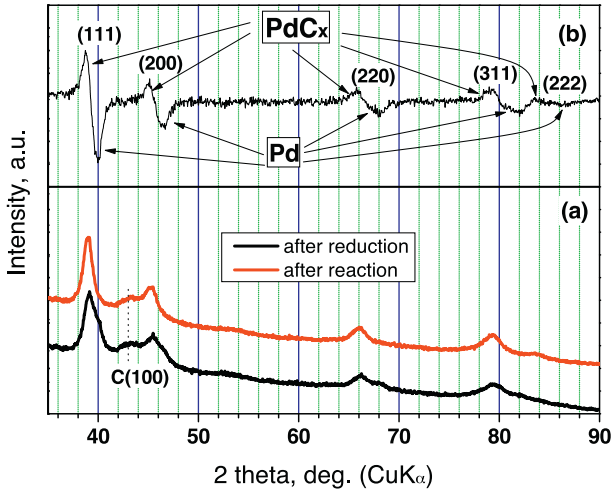

Fig. 5. XRD profiles of reduced and post-reaction Pd80Au20-RD catalyst (a) and difference (post-reaction–reduced) XRD spectrum (b). Basic reflections from Pd and PdC_x fcc phases are marked.

reaction temperature. It is known that poorly dispersed gold is not efficient in hydrogen activation, so its surface must by quickly blocked by nonreactive species conceivably formed from adsorbed CCl_4. Preparation of less metal loaded Au/Sibunit catalyst (2 wt.%) by using the same technique and pretreatment (400 °C reduction) brought about very modest improvement in the catalytic behavior (~1% conversion with methane as a dominant product), justified by the presence of still large metal crystallites (~13 nm, Fig. 6). This is in line with previously reported catalytic activity of Au/Al_2O_3 catalysts, which were only slightly active in HdCl of 2,4-dichlorophenol, generating 2-chlorophenol (2-CP) as the sole product [86]. Further attempts to prepare a more dispersed gold catalysts were not undertaken after inspecting available literature on this subject. Highly dispersed gold catalysts are relatively easy to prepare using oxidic supports, like Al_2O_3, TiO_2, Fe_2O_3, precipitation-deposition methods and low metal loadings. With carbon supports it is not easy because carbon materials are reducing agents, and they can react with Au^{3+} to form large gold particles during synthesis [87,88]. Small gold particles supported on carbon are attainable by using polymer (PVA, PVP)-protected Au sols [87,89,90] and very careful temperature pretreatment used for polymer removal.

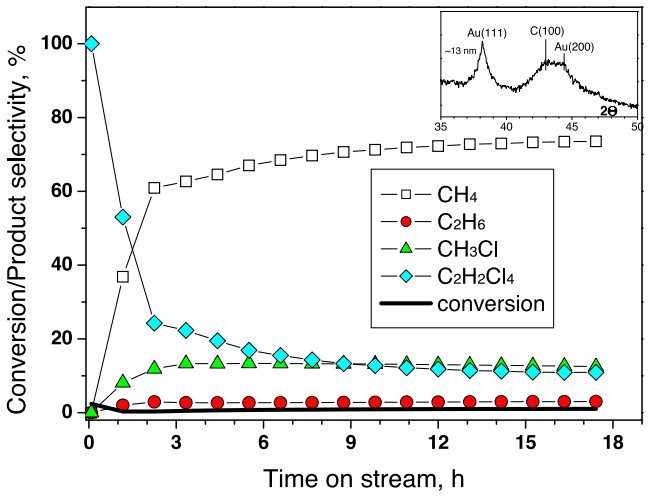

Fig. 6. Time on stream behavior of 2 wt.% Au/Sibunit carbon catalyst in HDC of CCl_4: Reaction temperature 90 °C, H_2/CCl_4 = 14, catalyst weight 0.24 g. Inset: XRD profile of this catalyst after reduction at 400 °C for 2 h.

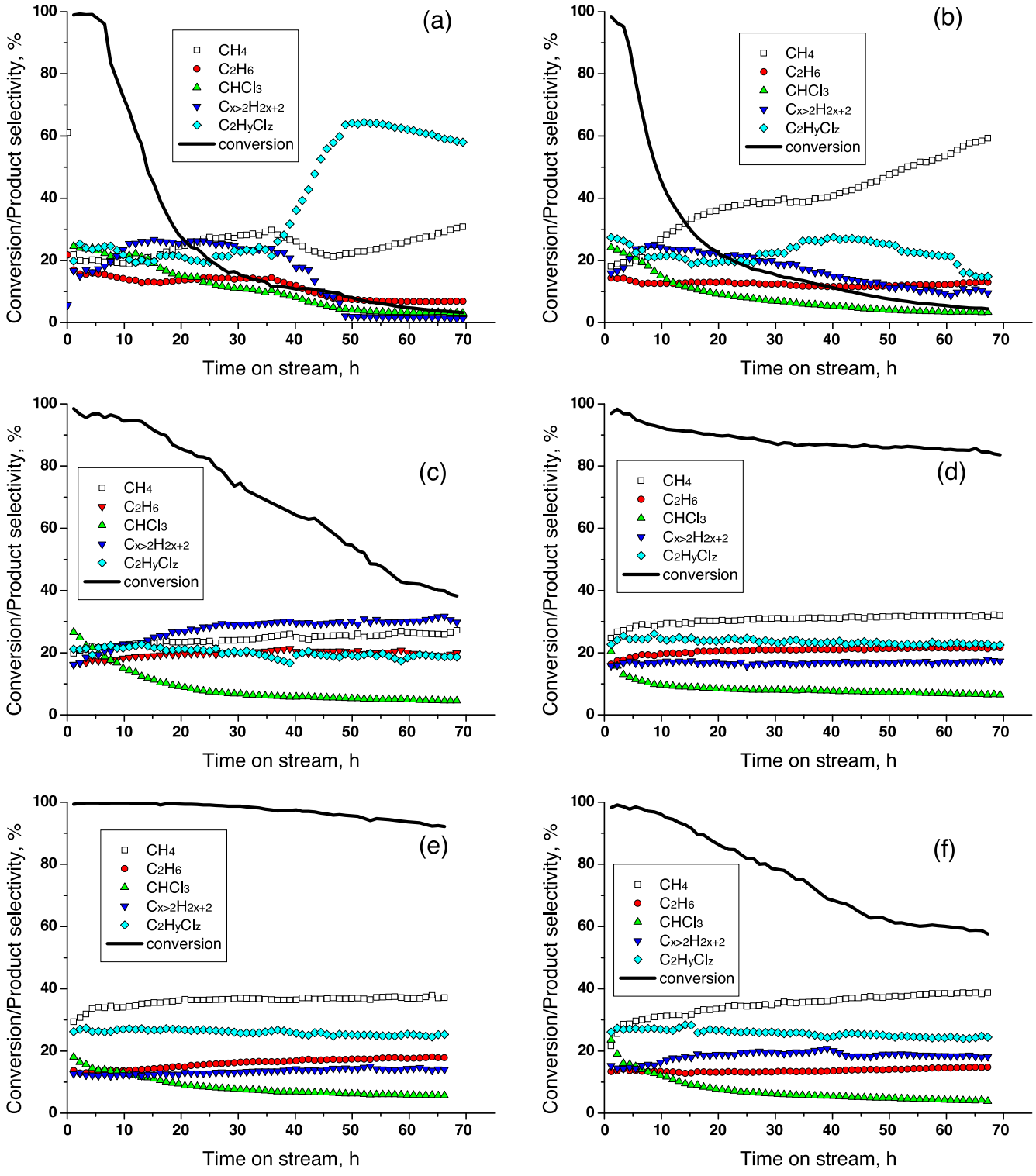

Fig. 7. Time on stream behavior of Pd-Au/Sibunit carbon catalysts in HDC of CCl_4: (a) Pd100, (b) Pd60Au40-SI, (c) Pd82Au18-RD, (d) Pd71Au29-RD, (e) Pd62Au38-RD, (f) Pd49Au51-RD. Reaction temperature 90 °C, H_2/CCl_4 = 14, catalyst weight 0.24 g.

Used in this work the temperature of catalyst reduction 400 °C (to facilitate better Pd-Au alloying) appears to high for maintaining high dispersion of gold, as can be judged from the work of Dash et al. [90]. To provide the same state of activated carbon surface (acidity, pore structure, etc.) we decided to keep firmly the severity of reduction condition. Therefore, a highly desirable investigation of CCl_4 HdCl activity of small Au particles has to be suspended to future studies. Interestingly enough, hematite-supported very small gold particles were recently found very active in HdCl of 2,4-dichlorophenol [91].

Fig. 6 shows the time on stream behavior of all tested Pd and Pd-Au catalysts. It is evident that the performance of Pd100 suffers from rapid deactivation, in line with other reports [6–9,12–16]. In addition, the product distribution changes during long term (~70 h) experiments: dimeric $C_2H_xCl_y$ products start to play a dominant role, when the catalyst is gradually more deactivated

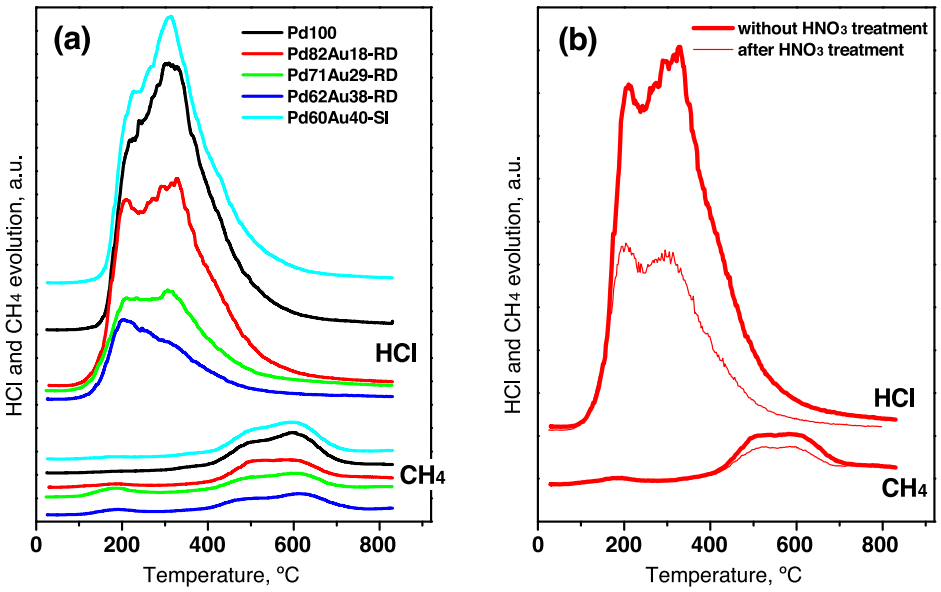

Fig. 8. Temperature programmed hydrogenation profiles of postreaction deposits from Sibunit carbon-supported Pd and Pd-Au catalysts: (a) HCl (m/z 36) and methane (m/z 16) evolution (b); comparison between carbon- and chlorine-containing deposits from HNO_3 washed and unwashed Pd82Au18-RD catalyst. In (b) the Y-axis is expanded by factor of 2 compared to (a).

(Fig. 6a). A similar situation is observed for the Pd60Au40-SI catalyst (Fig. 5b), which showed practically no Pd-Au alloying (i.e. presence of big Pd10Au90 crystallites and very small Pd particles, previous subsection and Table 1). It is clear that the initial course of reaction (~10–30 h) must be largely regulated by the presence of unalloyed palladium, with minor contribution of very Au-rich phase. The only difference between the behavior of Pd100 and Pd60Au40-SI is observed in product selectivities. After ~30–40 h of time on stream, evolution of dimeric $C_2H_yCl_z$ begins to dominate for Pd100, whereas methane formation contributes most for Pd60Au40-SI, i.e. adopting the characteristic of Au/C catalyst (Fig. 5a). It appears that after an initial period of relatively effective action, the unalloyed palladium drastically loses its performance, so that the action of initially disregarded Au-rich alloys starts to be more significant. Being less than pure palladium blocked by coke, the surface of Pd-Au appears to be less suited for producing dimeric

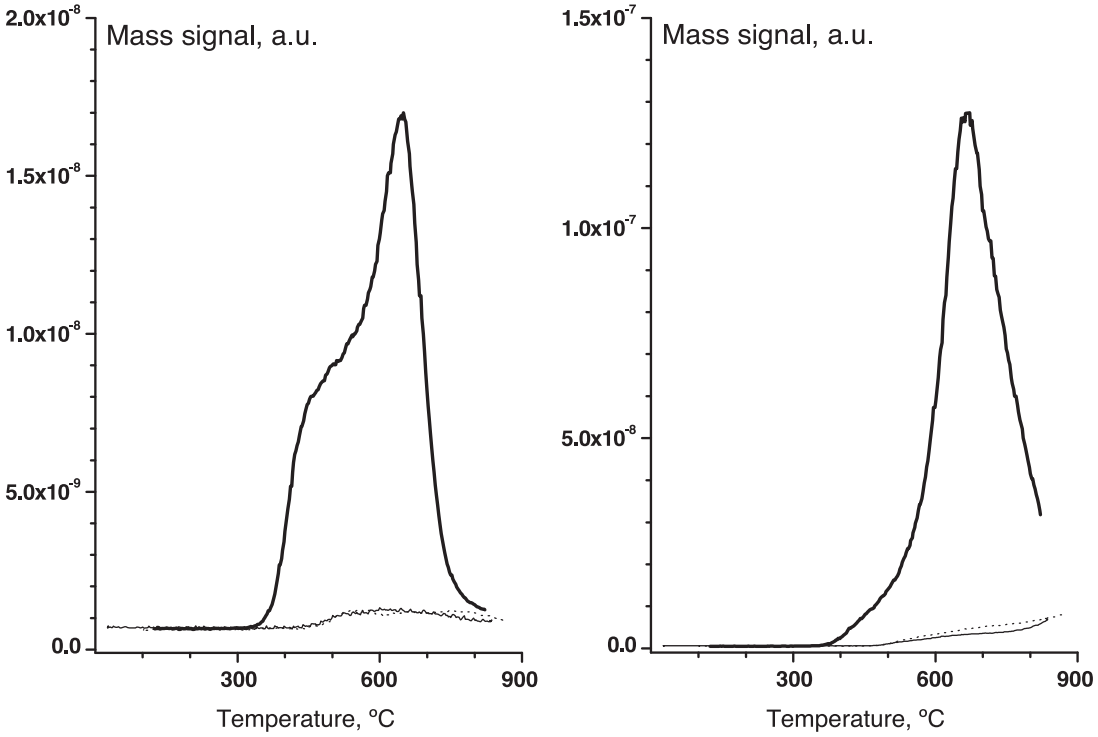

Fig. 9. Temperature-programmed desorption profiles from reduced Pd100/Sibunit carbon catalyst samples. (a) CO_2 evolution, (b) CO evolution. HNO_3-untreated Pd100/C thin solid lines, HNO_3-treated Pd100/C-thin dotted lines. For comparison respective profiles for Norit carbon GF40, pretreated in Ar at 500 °C (thick lines), were taken from Ref. [100]. All samples ~0.45 g.

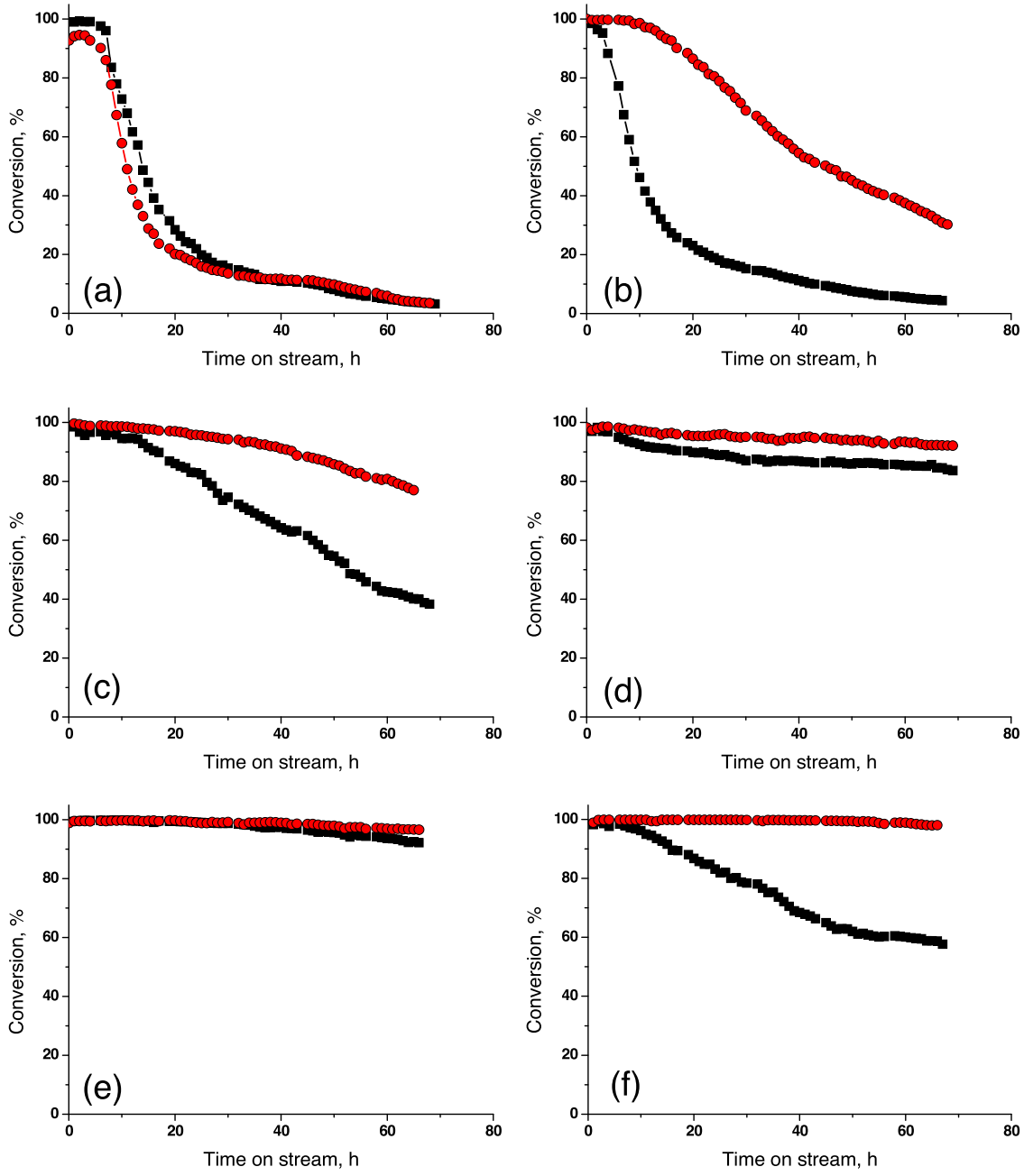

Fig. 10. The effect of HNO_3 treatment on the stability of Pd-Au/Sibunit catalysts. Only conversion changes are marked. (a) Pd100, (b) Pd60Au400-SI, (c) Pd82Au18-RD, (d) Pd71Au29-RD, (e) Pd62Au38-RD, (f) Pd49Au51-RD. Reaction conditions as in Fig. 7.

$C_2H_yCl_z$ species, although it is still efficient in C–Cl splitting and hydrogenation of surface carbon species.

For the bimetallic Pd-Au catalysts (excluding the SI catalyst) changes in overall conversion and product selectivities are rather mild, although different for particular catalysts. General conclusion is that introduction of gold to palladium results in a considerable improvement in the catalytic behavior (Fig. 6). Both the overall activity, catalyst stability and product selectivity (for hydrocarbons regarded as desired products, Table 2) of palladium are positively influenced by gold addition.

3.2.2. *Synergistic effects*

Initial conversion levels of HdCl of CCl_4 on all tested catalysts were very high, close to 100%. This limitation does not allow for discussion in the light of initial activity. Therefore, possible synergistic effects associated with Pd-Au alloying will be discussed in terms of final activities and product selectivities. As mentioned earlier, all the tested catalysts deactivated on stream, however, this effect was most marked for Pd100 and Pd60Au40-SI, which contained a large number of small unalloyed palladium particles. The positive effect of gold was seen for the rest of Pd-Au catalysts, which exhibited much better, although not equal resistance to deactivation (Fig. 6). A comparison of these results with data on the phase composition of Pd-Au/C (Table 1) leads to a direct correlation between resistance for deactivation with the composition of the alloy of Pd-Au. In this respect, the best catalysts appeared Pd62Au38-RD and Pd71Au29-RD, which contained 90 and 80% of alloyed palladium. They were even better than Pd49Au51-RD, which apart from having Au-rich alloy phase (65 at.% Au) retained very small (i.e. quickly deactivating) Pd particles. Its time on stream behavior resembles to a certain extent the performance of the previous discussed Pd60Au40-SI catalyst (subsection 2.3.1) with the dominant role of

the palladium during the first 40 h reaction (characterized by rapid deactivation), followed by a slower decline in conversion (Fig. 6f).

Final, nearly stable CCl_4 conversions, all below 100% level, enabled estimation of turnover frequencies (based on CO/Pd values from Table 1). The TOF values presented in Table 1 indicate again that Pd62Au38-RD and Pd71Au29-RD are the best catalysts. Therefore it appears that introduction of 30–40 at.% Au to palladium results in optimal catalytic performance in HdCl of CCl_4.

Apparent activation energies (E_A's) calculated from TOF data (at 90, 80 and 70 °C; TOFs at 80 and 70 °C not presented in Table 2) are in the last column of Table 2. Relatively small errors in E_A ($\pm\Delta E_A$) result from good straight lines representing Arrhenius plots, i.e. without detectable "bending" at highest reaction temperatures. It supports our considerations about apparent absence of diffusional problems (section 2.2). Much lower apparent activation energies found for Pd62Au38-RD and Pd71Au29-RDagain indicate their superior character.

Table 2 collects the selectivity data for all tested catalysts. It is seen that although gold itself is inactive in HdCl of CCl_4, its addition to Pd vastly increases the selectivity towards hydrocarbons, which are considered as the most desired reaction products. It should also be noticed that longer than methane hydrocarbons should be even more preferred reaction products. Summing the selectivities for ethane and longer hydrocarbons shows the superiority of reasonably well-mixed Pd-Au catalysts with produce $C_{>2}$ hydrocarbons with the selectivity between 31 and 49.7%, compared to only 8.1% for Pd100 and 22.5% for inhomogeneous Pd60Au40-SI.

Temperature programmed hydrogenation (TPH) of used catalysts (Fig. 8a) shows that post-reaction deposits have mainly chlorine-containing species and smaller amounts of carbonaceous deposits, which are hydrogenated off at higher temperature (>400 °C). The Pd-Au catalysts, which also showed better stability, especially Pd62Au38-RD and Pd71Au29-RD, contained less deposit. However, when Pd-Au alloying practically does not exist (as in the case of Pd60Au40-SI) and deactivation reaches a similar level as for Pd100 (Fig. 6), the amounts of post-reaction deposits are similar in both cases. Pd100 and Pd60Au40-SI (i.e. poorly mixed Pd-Au alloy catalyst) liberate the largest amounts of HCl, although according to a simplified stoichiometry of CCl_4 hydrodechlorination ($CCl_4 + 4H_2 = CH_4 + 4HCl$) and rapid catalyst deactivation, they should produce the smallest amounts of HCl. Chloriding metal surface does not seem a critical cause of catalyst deactivation because 1 h hydrogen treatment of post-reaction catalysts at 350 °C (i.e. higher than T_{max} for HCl evolution during TPH run) does not reactivate them. Therefore, it appears that deactivation by carbonaceous deposits, although much less plentiful than surface chloride species, cannot be neglected, especially when their removal needs higher hydrogenation temperatures, ~500 °C (Fig. 7). Methane evolution at ~600 °C and above in the TPH profiles would also originate from gasification of Sibunit carbon, facilitated by the presence of metal.

It was suggested that the presence of surface chloride species, which is formed as intermediate during dissociative adsorption of CCl_4, oxidizes palladium on the catalytic surface generating active sites of oligomerization [9]. It appears that introducing gold to palladium must decrease the affinity to chloride species. A direct comparison of free energy of formation for gold and palladium chlorides [92] implies much weaker metal–Cl bond in the case of gold. A higher activation energy formonometallic Pd100 (~52 vs. ~15–30 kJ/mol for the bimetallics, Table 2) would suggest that the removal of surface chlorine (as HCl by interaction with hydrogen which is in excess in the gas phase) is more difficult for Pd only surface than for bimetallic Pd–Au surface. Such explanation is in a qualitative agreement with the mechanism of hydrodechlorination suggested by Chen et al. [93] who studied the reaction kinetics of hydrodechlorination for a series of $CH_{4-x}Cl_x$ (x = 1–4) compounds on a Pd/carbon catalyst and arrived with suggested reaction mechanism considering irreversible scission of the first C–Cl bond in the molecularly adsorbed molecule as the rate-determining step. Gas phase H_2 and HCl were suggested to be in equilibrium with surface H and Cl; and adsorbed Cl as the most abundant surface intermediate. The overall hydrodechlorination reaction rate, $r = kK_{R-Cl}[R\text{-}Cl]/(1 + K_{HCl}[HCl]/K_{H_2}^{1/2}[H_2]^{1/2})$ contains in the denominator the factor associated with HCl, resulted from surface coverage by Cl species (K's are respective equilibrium constants and k is the rate constant of the rate determining step).

Although we have not studied the reaction kinetics in much detail (no partial pressure study), it appears that a higher apparent activation energy may result from surface occupation by chloride species more strongly bonded to palladium than to Pd-Au surface. Also, much smaller amounts of surface chlorine species on the surface of Pd-Au catalysts during HdCl would explain their better selectivity to hydrocarbons and not to chlorine-containing organic compounds.

However, still another explanation should be considered. Initial activity of monometallic palladium is probably at least as high as that of bimetallic Pd-Au alloys. The problem is that palladium quickly deactivates in time on stream. The reason of such situation would be that the C1 adspecies which are formed after stripping off chlorine from CCl_4 molecules swiftly migrate into palladium bulk. As long as such "sink" is not full (saturation up to $PdC_{0.13-0.15}$), the Pd surface still keeps its characteristics, i.e. high hydrodechlorination activity. This stage maintains for ~10–12 h (Fig. 6). However, when all palladium material turns PdC_x, its surface becomes less active in hydrogen dissociation. Being deprived of active hydrogen, dissociatively adsorbed CCl_4 is not easily hydrogenized and the reaction slows down. This situation leads also to the formation of less active dimeric species and deposition of coke, containing both carbon and chlorine species. This would also contribute to higher values of apparent activation energy for Pd100. For Pd-Au alloys carbiding does not take place, so the surface is less covered by C1 species, leaving more room for hydrogen chemisorption, and, in effect, for hydrodechlorination.

In general, the catalytic synergy when Pd and Au metals are alloyed would be ascribed to a ligand (electronic) or ensemble (geometric) effect. It is difficult to decide if one of them (or both) are applicable in our case, because we do not dispose of any data on surface composition of our catalysts, especially those established during CCl_4 hydrodechlorination.

The explanation via direct charge transfer (ligand effect) brings about the Pd d band to be more filled, moving the d-band center away from the Fermi level, what makes Pd more "atomic like" therefore binding reactants and products more weakly [33]. This would explain better, compared with pure Pd, resistance to deactivation of Pd-Au catalysts. However, we also believe that although gold itself is not active in the reaction because of inability to dissociate hydrogen (see 3.2.1), it is still able to chemisorb tetrachloromethane with possible splitting of several C–Cl bonds. But without surface palladium species further reaction stops, because of shortage of active hydrogen. So, surface palladium species furnish active hydrogen needed for the reaction and product desorption. Such bifunctional mechanism resembles the mechanism suggested in our recent paper on CCl_4 hydrodechlorination on Pd-Cu/Sibunit catalysts [67].

3.2.3. Upgrading Pd-Au catalysts by leaching unalloyed palladium particles

As mentioned earlier, palladium is very active and selective catalyst in HdCl of CCl_4, but its stability is rather poor.

Table 3
Metal leaching from Pd49Au51-RD catalyst by dissolution in 10% nitric acid.

Catalyst treatment	wt.% Pd		wt.% Au	
	AAS	ICP	AAS	ICP
After reduction	2.72	2.78	5.24	4.92
20 h HNO_3 leach	1.75	1.77	5.18	4.97

Similar undesirable effect is observed for the bimetallic Pd-Au catalysts which contained significant amounts of unalloyed palladium. Therefore, in an effort to improve the catalytic behaviour of the tested materials we decided to get rid of this unhelpful component. It could be accomplished through the use of cold dilute nitric acid (10%), in the hope that the leaching operation will not lead to the removal of gold or palladium from Pd-Au particles. Highly concentrated HNO_3 (65%) was not considered because its action would result in a significant dealloying (Pd removal from Pd-Au) and development of extensive porosity of a residual alloy phase [94]. We also thought that even if it were possible to develop alloy particle coarsening and porosity under the action of dilute nitric acid, such effects should be relaxedduring subsequent hydrogen treatment at 400 °C. Leaching procedures took 10 or 20 h, depending on the amount of unalloyed palladium in pre-reduced catalysts [95], i.e. the relatively well-homogenized Pd71Au29-RD and Pd62Au38-RD were treated 10 h and the remaining catalysts, i.e. Pd100 and Pd-Au/C characterized by a lesser degree of alloying, were treated 20 h.It should be added that the metal crystallite sizes as judged from XRD were practically unchanged after HNO_3 treatment and rereduction at 400 °C. It is well known that HNO_3 treatment of carbons results in development of oxygen-containing functional groups (carbonyl, carboxyl, etc.) which would contribute to surface acidity [96] and desorb primarily as CO_2 and CO in TPD runs. Although, inspection of available literature leads to conclusion that H_2 treatment of HNO_3-treated Pd/carbon catalysts at elevated temperature drastically reduces the content of such functional groups [97–99], we decided to check this for HNO_3-treated and untreated Pd-Au catalyst. Fig. 9 shows respective CO_2 and CO evolutions, which are similar and insubstantial in comparison to the TPD results for commercial carbon Norit G40, used in our previous study [100], indicating that after hydrogen treatment at 400 °C for 2 h, HNO_3-untreated and HNO_3-treated Sibunit carbon samples carry only very limited and similar amounts of oxygen-containing groups which would contribute to surface acidity. This result allows us to ignore possible support effects and discuss changes in the catalytic behavior in terms of modification of the active phase generated by HNO_3-treatment.

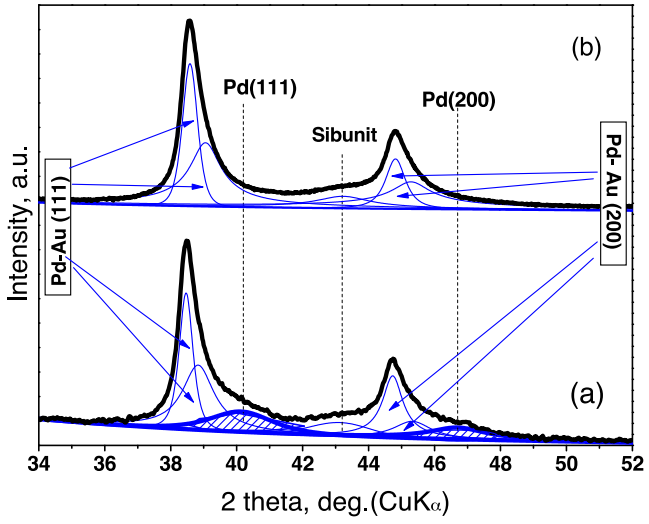

Fig. 11. XRD profiles of Pd49Au51-RD catalyst after reduction (a) and after HNO_3 treatment (b). The obtained XRD profiles were fitted to an analytical function of the PEARSON-VII type (see Experimental). Bottom profile shows nonnegligible amounts of highly dispersed unalloyed palladium which is effectively removed by HNO_3 treatment.

The monometallic Pd100/Sibunit does not noticeably change its catalytic behavior after HNO_3 leaching (Fig. 10a), showing only somewhat faster deactivation. It is in line with somewhat diminished Pd loading after leach (~2 wt.% instead of 2.8 wt.%). But for the rest of tested catalyst the effect of leaching is remarkable, because all the materials turned out to be more resistant to deactivation (Fig. 10b–f). Changes in the catalyst composition and homogeneity are exemplified for Pd62Au38-RD catalyst. Table 3 shows the results of chemical analysis, indicating that the catalyst is deprived a considerable part of palladium, whereas the content of gold is practically unchanged. XRD profiles (Fig. 11) also reveal the loss of a considerable part of unalloyed highly dispersed palladium species.

Improvement of the catalyst's performance by acid leach corresponds well with lesser amounts of post-reaction deposits, as it is shown for Pd82Au18-RD catalyst (Fig. 8b).

4. Conclusions

1. Pd-Au/C preparation by sequential impregnation of Pd/C with gold salt leads to poor alloy homogeneity, whereas impregnation of a pre-reduced Pd/C gives a significant (but not complete) metal alloying.
2. Activated carbon-supported Pd-Au catalysts show much better performance than the monometallic Pd samples in hydrodechlorination of tetrachloromethane, but Pd-Au intermixing is crucial to obtain this synergistic effect.
3. Higher overall activity and better selectivity towards hydrocarbon products achieved for the bimetallic catalysts are attributable to the improved deactivation resistance associated with reduced retention of surface chlorine and carbonaceous species during hydrodechlorination.
4. Upgrading insufficiently intermixed Pd-Au catalysts can be achieved as a result of selective removal of unalloyed palladium particles, which are not resistant to deactivation. This can be achieved by dissolution in dilute nitric acid.

Acknowledgements

This work was supported by the Polish National Science Centre within Research Project DEC-2011/01/B/ST5/03888 and also, in part, by the grant from the Polish Ministry of Science and Higher Education - decision 753/N-COST/2010/0.

References

[1] V.I. Kovalchuk, J.L. d'Itri, Appl. Catal. A: Gen. 271 (2004) 13–25.
[2] M.A. Keane, ChemCatChem 3 (2011) 800–821.
[3] Z.C. Zhang, B.C. Beard, Appl. Catal. A: Gen. 174 (1998) 33–39.
[4] M.T. Holbrook, J.D. Myers, US Patent No. 2007/0225530 A1.
[5] M. Bonarowska, Z. Kaszkur, L. Kępiński, Z. Karpiński, Appl. Catal. B: Environ. 99 (2010) 248–256.
[6] E.S. Lokteva, V.I. Simagina, E.V. Golubina, I.V. Stoyanova, V.V. Lunin, Kinet. Catal. 41 (2000) 776–781.
[7] E.S. Lokteva, V.V. Lunin, E.V. Golubina, V.I. Simagina, M. Egorova, I.V. Stoyanova, Stud. Surf. Sci. Catal. 130 (2000) 1997–2002.
[8] V. Dal Santo, C. Dossi, S. Recchia, P.E. Colavita, G. Vlaic, R. Psaro, J. Mol. Catal. A: Chem. 182–183 (2002) 157–166.
[9] E.V. Golubina, E.S. Lokteva, V.V. Lunin, A.O. Turakulova, V.I. Simagina, I.V. Stoyanova, Appl. Catal. A: Gen. 241 (2003) 123–132.
[10] B. Imre, I. Hannus, I. Kiricsi, J. Mol. Struct. 744–747 (2005) 501–506.
[11] I. Hannus, J. Halász, J. Japan Petrol. Inst. 49 (2006) 105–113.
[12] B. Szczepaniak, J. Góralski, J. Grams, T. Paryjczak, Przem. Chem. 85 (2006) 764–765.
[13] B. Szczepaniak, J. Góralski, J. Grams, T. Paryjczak, Pol. J. Environ. Stud. 15 (2006) 161–164.

[14] J. Grams, J. Góralski, B. Szczepaniak, Russ. J. Phys. Chem. A 81 (2007) 1515–1520.
[15] J. Goralski, V.S. Federyaeva, R.F. Vitkovskaya, M. Szinkowska, Russ. J. Appl. Chem. 85 (2012) 598–603.
[16] L. Prati, M. Rossi, Appl. Catal. B: Environ. 23 (1999) 135–142.
[17] B. Coq, G. Ferrat, F. Figueras, J. Catal. 101 (1986) 434–445.
[18] B. Coq, J.M. Cognion, F. Figueras, D. Tournigant, J. Catal. 141 (1993) 21–33.
[19] Z. Karpinski, K. Early, J.L. d'Itri, J. Catal. 164 (1996) 378–386.
[20] W. Juszczyk, A. Malinowski, Z. Karpinski, Appl. Catal. A: Gen. 166 (1998) 311–319.
[21] A.L. Dantas Ramos, P. da Silva Alves, D.A.G. Aranda, M. Schmal, Appl. Catal. A: Gen. 277 (2004) 71–81.
[22] C.A. Gonza´lez Sa´nchez, C.O. Maya Patiño, C. Montes de Correa, Catal. Today 133–135 (2008) 520–525.
[23] S. Ordóñez, E. Díaz, R.F. Bueres, E. Asedegbega-Nieto, H. Sastre, J. Catal. 272 (2010) 158–163.
[24] S. Jujjuri, M.A. Keane, Chem. Eng. J. 157 (2010) 121–130.
[25] E. Díaz, L. Faba, S. Ordóñez, Appl. Catal. B: Environ. 104 (2011) 415–417.
[26] M.A. Aramendia, V. Borau, I.M. Garcia, C. Jimenez, A. Marinas, J.M. Marinas, F.J. Urbano, J. Catal. 187 (1999) 392.
[27] F.J. Urbano, J.M. Marinas, J. Mol. Catal. A: Chem. 173 (2001) 329–345.
[28] H.C. Choi, S.H. Choi, O.B. Yang, J.S. Lee, K.H. Lee, Y.G. Kim, J. Catal. 161 (1996) 790–797.
[29] L. Gómez-Sainero, X. Seoane, J. Fierro, A. Arcoya, J. Catal. 209 (2002) 279–288.
[30] M.A. Álvarez-Montero, L.M. Gómez-Sainero, M. Martín-Martínez, F. Heras, J.J. Rodriguez, Appl. Catal. B: Environ. 96 (2010) 148–156.
[31] J.A. Baeza, L. Calvo, M.A. Gilarranz, A.F. Mohedano, J.A. Casas, J.J. Rodriguez, J. Catal. 293 (2012) 85–93.
[32] S. Ordóñez, E. Díaz, R.F. Bueres, E. Asedegbega-Nieto, H. Sastre, J. Catal. 272 (2010) 158–168.
[33] Z.C. Zhang, B.C. Beard, Appl. Catal. A: Gen. 188 (1998) 229–240.
[34] J.W. Bae, I.G. Kim, J.S. Lee, K.H. Lee, E.J. Jang, Appl. Catal. A: Gen. 240 (2003) 129–142.
[35] J.W. Bae, J.S. Lee, K.H. Lee, Appl. Catal. A: Gen. 334 (2008) 156–167.
[36] E.-J. Shin, A. Spiller, G. Tavoularis, M.A. Keane, Phys. Chem. Chem. Phys. 1 (1999) 3173–3181.
[37] S. Ordóñez, F.V. Díez, H. Sastre, Appl. Catal. B: Environ. 31 (2001) 113–122.
[38] K.A. Frankel, B.W.-L. Jang, J.J. Spivey, G.W. Roberts, Appl. Catal. A: Gen. 205 (2001) 263–278.
[39] K.A. Frankel, B.W.-L. Jang, G.W. Roberts, J.J. Spivey, Appl. Catal. A: Gen. 209 (2001) 401–413.
[40] S.Y. Kim, H.C. Choi, O.B. Yanga, K.H. Lee, J.C. Lee, J.G. Kim, J. Chem. Soc. Chem. Commun. (1995) 2169–2170.
[41] D.J. Moon, M.J. Chung, K.Y. Park, S.I. Hong, Appl. Catal. A: Gen. 168 (1998) 159–170.
[42] E. López, S. Ordóñez, F.V. Díez, Appl. Catal. B: Environ. 62 (2006) 57–65.
[43] J. Grams, J. Góralski, P. Kwintal, Int. J. Mass Spectrom. 292 (2010) 1–6.
[44] F. Gao, D.W. Goodman, Chem. Soc. Rev. 41 (2012) 8009–8020.
[45] A.M. Venezia, V. La Parola, G. Deganello, B. Pawelec, J.L.G. Fierro, J. Catal. 215 (2003) 317–325.
[46] M.O. Nutt, J.B. Hughes, M.S. Wong, Environ. Sci. Technol. 39 (2005) 1346–1353.
[47] M.O. Nutt, K.N. Heck, P. Alvarez, M.S. Wong, Appl. Catal. B: Environ. 69 (2006) 115–125.
[48] M.S. Wong, P.J.J. Alvarez, Y.-L. Fang, N. Akçin, M.O. Nutt, J.T. Miller, K.N. Heck, J. Chem. Technol. Biotechnol. 84 (2009) 158–166.
[49] K.N. Heck, M.O. Nutt, P. Alvarez, M.S. Wong, J. Catal. 267 (2009) 97–104.
[50] Y.L. Fang, N. Guo, K.N. Heck, P.J.J. Alvarez, M.S. Wong, ACS Catal. 1 (2011) 128–138.
[51] Y.L. Fang, J.T. Miller, N. Guo, K.N. Heck, P.J.J. Alvarez, M.S. Wong, Catal. Today 96 (2011) 96–102.
[52] L.A. Pretzer, H.J. Song, Y.-L. Fang, Z. Zhao, N. Guo, T. Wuc, I. Arslan, J.T. Miller, M.S. Wong, J. Catal. 298 (2013) 206–217.
[53] J.C. Velázquez, S. Leekumjorn, Q.X. Nguyen, Y.-L. Fang, K.N. Heck, G.D. Hopkins, M. Reinhard, M.S. Wong, AIChE J. 59 (2013) 4474–4482.
[54] Z. Wu, C. Sun, Y. Chai, M. Zhang, RSC Adv. 1 (2011) 1179–1182.
[55] M. Bonarowska, J. Pielaszek, V.A. Semikolenov, Z. Karpiński, J. Catal. 209 (2002) 528–538.
[56] E.G. Allison, G.C. Bond, Catal. Rev. 7 (1973) 233–289.
[57] V. Ponec, G.C. Bond, Catalysis by Metals and Alloys, Elsevier, Amsterdam, 1996.
[58] G.J. Hutchings, Chem. Commun. (2008) 1148–1164.
[59] E.V. Golubina, E.S. Lokteva, T.S. Lazareva, B.G. Kostyuk, V.V. Lunin, V.I. Simagina, I.V. Stoyanova, Kinet. Catal. 45 (2004) 183–188.
[60] B. Heinrichs, P. Delhez, J.-P. Schoebrechts, J.-P. Pirard, J. Catal. 172 (1997) 322–335.
[61] S. Lambert, B. Heinrichs, A. Brasseur, A. Rulmont, J.-P. Pirard, Appl. Catal. A: Gen. 270 (2004) 201–208.
[62] S. Lambert, F. Ferauche, A. Brasseur, J.-P. Pirard, B. Heinrichs, Catal. Today 100 (2005) 283–289.
[63] N. Job, B. Heinrichs, F. Ferauche, F. Noville, J. Marien, J.-P. Pirard, Catal. Today 102–103 (2005) 234–241.
[64] N. Job, B. Heinrichs, S. Lambert, J.-P. Pirard, J.-F. Colomer, B. Vertruyen, J. Marien, AIChE J. 52 (2006) 2663–2676.
[65] A. Śrębowata, W. Lisowski, J.W. Sobczak, Z. Karpiński, Catal. Today 175 (2011) 576–584.
[66] M. Lu, J. Sun, D. Zhang, M. Li, J. Zhu, Y. Shan, Reac. Kinet. Mech. Cat. 100 (2010) 99–103.
[67] M. Bonarowska, O. Machynskyy, D. Łomot, E. Kemnitz, Z. Karpiński, Catal. Today (2014), http://dx.doi.org/10.1016/j.cattod.2014.01.029
[68] M.A. Keane, S. Gómez-Quero, F. Cárdenas-Lizana, W. Shen, ChemCatChem 1 (2009) 270–278.
[69] V.B. Fenelonov, V.A. Likholobov, A.Yu. Derevyankin, M.S. Mel'gunov, Catal. Today 42 (1998) 341–345.
[70] A. Śrębowata, W. Juszczyk, Z. Kaszkur, J.W. Sobczak, L. Kępiński, Z. Karpiński, Appl. Catal. A: Gen. 319 (2007) 181–192.
[71] M. Gurrath, T. Kuretzky, H.P. Boehm, L.B. Okhlopkova, A.S. Lisitsyn, V.A. Likholobov, Carbon 38 (2000) 1241–1255, especially the entry in second row and last column in Table 3, on p. 1245.
[72] S. Ichikawa, H. Poppa, M. Boudart, J. Catal. 91 (1985) 1–10.
[73] N. Krishnankutty, M.A. Vannice, Appl. Catal. A: Gen. 155 (1995) 312–326.
[74] N. Krishnankutty, J. Li, M.A. Vannice, Appl. Catal. A: Gen. 173 (1998) 137–144.
[75] A. Sárkány, A. Horváth, A. Beck, Appl. Catal. A: Gen. 229 (2002) 117–125.
[76] Y.L. Lam, M. Boudart, J. Catal. 50 (1977) 530–540.
[77] J.A. McCaulley, Phys. Rev. B 47 (1993) 4873–4879.
[78] M. Maciejewski, A. Baiker, Pure Appl. Chem. 67 (1995) 1879–1884.
[79] E.J.A.X. van de Sandt, A. Wiersma, M. Makkee, H. van Bekkum, J.A. Moulijn, Catal. Today 35 (1997) 163–170.
[80] E.J.A.X. van de Sandt, A. Wiersma, M. Makkee, H. van Bekkum, J.A. Moulijn, Appl. Catal. A: Gen. 155 (1997) 59–73.
[81] A. Malinowski, W. Juszczyk, M. Bonarowska, J. Pielaszek, Z. Karpiński, J. Catal. 177 (1998) 153–163.
[82] M. Öcal, M. Maciejewski, A. Baiker, Appl. Catal. B: Environ. 21 (1999) 279–289.
[83] A. Morato, C. Alonso, F. Medina, Y. Cesteros, P. Salagre, J.E. Sueiras, D. Tichit, B. Coq, Appl. Catal. B: Environ. 32 (2001) 167–179.
[84] M. Bonarowska, A. Malinowski, W. Juszczyk, Z. Karpiński, Appl. Catal. B: Environ. 30 (2001) 187–193.
[85] Y.-F. Han, D. Kumar, C. Sivadinarayana, A. Clearfield, D.W. Goodman, Catal. Lett. 94 (2004) 131–134.
[86] M.A. Keane, S. Gómez-Quero, F. Cárdenas-Lizana, W.Q. Shen, ChemCatChem 1 (2009) 270–278.
[87] L. Prati, G. Martra, Gold Bull. 32 (1999) 96–101.
[88] Z. Ma, S. Dai, Nano Res. 4 (2011) 3–32.
[89] W.C. Ketchie, Y.-L. Fang, M.S. Wong, M. Murayama, R.J. Davis, J. Catal. 250 (2007) 94–101.
[90] P. Dash, T. Bond, C. Fowler, W. Hou, N. Coombs, R.W.J. Scott, J. Phys. Chem. C 113 (2009) 12719–12730.
[91] S. Gómez-Quero, F. Cárdenas-Lizana, M.A. Keane, J. Catal. 303 (2013) 41–49.
[92] I. Barin, in: Thermochemical Data of Pure Substances, 3rd ed., VCH, Weinheim, 1995.
[93] N. Chen, R.M. Rioux, L.A.M.M. Barbosa, F.H. Ribeiro, Langmuir 26 (2010) 16615–16624.
[94] X. Wang, J. Sun, C. Zhang, T. Kou, Z. Zhang, J. Phys. Chem. C 116 (2012) 13271–13280.
[95] M. Bonarowska, Z. Karpiński, Polish Patent Pending, P-404842 (July 25, 2013).
[96] e. g. C. Moreno-Castilla, M.A. Ferro-Garcia, J.P. Joly, I. Bautista-Toledo, F. Carrasco-Marin, J. Rivera-Utrilla, Langmuir 11 (1996) 4386–4392.
[97] F. Coloma, A. Sepúlveda-Escribano, J.L.G. Fierro, F. Rodriguez-Reinoso, Appl. Catal. A: Gen. 150 (1997) 165–183.
[98] A. Sepúlveda-Escribano, F. Coloma, F. Rodríguez-Reinoso, Appl. Catal. A: Gen. 173 (1998) 247–257.
[99] H. Markus, A.J. Plomp, P. Mäki-Arvela, J.H. Bitter, D.Yu. Murzin, Catal. Lett. 113 (2007) 141–146.
[100] M. Bonarowska, W. Raróg-Pilecka, Z. Karpiński, Catal. Today 169 (2011) 223–231.